



Published in final edited form as:

Can J Chem. 2013 September 1; 91(9): 859–865. doi:10.1139/cjc-2012-0542.

Contribution of the empirical dispersion correction on the conformation of short alanine peptides obtained by gas-phase QM calculations

Elisa Fadda and

School of Chemistry, National University of Ireland, Galway, University Road, Galway, Ireland.

Robert J. Woods

School of Chemistry, National University of Ireland, Galway, University Road, Galway, Ireland; Complex Carbohydrate Research Center and Department of Chemistry, University of Georgia, Athens, GA 30602, USA

Abstract

In this work we analyze the effect of the inclusion of an empirical dispersion term to standard DFT (DFT-D) in the prediction of the conformational energy of the alanine dipeptide (Ala2) and in assessing the relative stabilities of short polyalanine peptides in helical conformations, i.e., α and 3_{10} helices, from Ala4 to Ala16. The Ala2 conformational energies obtained with the dispersion-corrected GGA functional B97-D are compared to previously published high level MP2 data. Meanwhile, the B97-D performance on larger polyalanine peptides is compared to MP2, B3LYP and RHF calculations obtained at a lower level of theory. Our results show that electron correlation affects the conformational energies of short peptides with a weight that increases with the peptide length. Indeed, while the contribution of vdW forces is significant for larger peptides, in the case of Ala2 it is negligible when compared to solvent effects. Even for short peptides, the inclusion of an empirical dispersion term greatly improves accuracy of DFT methods, providing results that correlate very well with the MP2 reference at no additional computational cost.

Keywords

alanine dipeptide; short polyalanine peptides; *ab initio* and DFT calculations; empirical dispersion-corrected DFT; peptides structure and stability; Ramachandran plot

Introduction

Mass spectrometry (MS) traditionally faces challenges when analysing mixtures of ions that all have equal molecular weights (isobaric mixtures), such as certain peptide sequences that arise from proteomic studies. A significant advance has been the development of ion-mobility spectrometry (IMS), which enables the separation of isobaric mixtures based on ion mobility. Ion mobility is proportional to the gas phase collisional cross-sectional area, which, for a protein, is typically assumed to be comparable to that for the corresponding

Corresponding authors: Elisa Fadda (elisa.fadda@nuigalway.ie) and Robert J. Woods (rwoods@ccrc.uga.edu).

protein crystal or NMR structure.¹ However, the gas-phase conformational preferences of peptides are unlikely to be similar to those for the same sequences in folded proteins.² Thus, the ability to independently predict the gas-phase conformations of peptides is essential for interpreting gas phase experimental data, such as from IMS-MS.

A logical approach to computing collisional cross-sectional areas would be to employ molecular dynamics (MD) simulations.^{3,4} However, common protein force fields have been validated principally in terms of their ability to reproduce solution phase properties of proteins. To assess the accuracy of existing protein force fields for predicting the conformational properties of peptides in the gas-phase, it is first necessary to establish a gas-phase structural and energetic reference set for polypeptides.

A wide range of ab initio methods have been used over the years to determine the conformational energies of minimal peptide models, such as the alanine dipeptide (Ala2).⁵⁻⁹ Moreover, advances in computer technology have allowed researchers to perform calculations with progressively larger basis sets and higher levels of theory.¹⁰⁻¹² Earlier work^{10,11,13-15} shows that the inclusion of electron correlation in QM calculations affects to different degrees the conformational propensity of small peptides and the stability of helical motifs. Accounting for electron correlation in an approximate fashion, less computationally expensive methods based on density functional theory (DFT) have often provided a speedy and reliable description of the conformational energy of minimal peptide models.^{11,16} Nevertheless, DFT and in particular LDA and GGA functionals fail when the contribution of long-range dispersion forces becomes essential for the correct description of molecular interactions.¹⁷⁻¹⁹ Over the past 10 years, QM methods that account explicitly for London or van der Waals dispersion (D) forces have been developed.²⁰⁻²³ Among those, the DFT-D approach^{15,20,22,24} is of particular interest, as it has been extremely successful in reproducing both theoretical and experimental results^{20,24-31} and in the description of systems of biological relevance^{20,22,32-35} at no additional computational cost than a standard DFT calculation. The DFT-D method consists in adding an C_6R^{-6} type empirical potential to the DFT energy, where R is the interatomic distance and C_6 are the dispersion coefficients.²⁰ In this work we compare the performance of Grimme's corrected GGA functional B97-D³⁵ to standard MP2 calculations¹¹ in defining the conformational preference of Ala2 in the gas phase. The B97-D functional was chosen based on its overall positive performance relative to B3LYP-D, BLYP-D, and PBE-D shown in earlier work.³⁵ Our results show that B97-D in combination with triple-zeta quality basis sets performs as well as the much more computationally expensive MP2 in evaluating the relative energies of all the minima found in the Ala2 conformational energy surface.

Electron correlation is known to play a significant role in stabilizing the conformation of peptides larger than the minimal Ala2 model.^{13,14} For peptides longer than 2 or 3 residues, higher correlated methods are still excessively expensive in terms of computational effort for routine applications. Because of that, one important issue that remains controversial is the relative stability of helical motifs, and in particular of α and 3_{10} helices, in medium to long peptides. These two types of helices differ in the hydrogen bonding pattern; the 3_{10} helix is characterized by hydrogen bonds between residues i and $i+3$, while the α helix by hydrogen bonds between residues i and $i+4$. Based on data deposited in the PDB, α helices

are virtually ubiquitous in proteins, containing between 4 and 40 residues with an average of 10 residues per helix. On the contrary, 3_{10} helices are quite uncommon in proteins, and when present they are relatively short. The longest 3_{10} helices ever identified are found in the voltage sensors of voltage gated channels, see for example ref. 36, and count 7 to 11 residues. B3LYP calculations^{37–39} on polyalanine peptides have shown that the stability order between α and 3_{10} helices in the gas phase is inverted relative to the evidence from the PDB. Indeed, 3_{10} helices are predicted to be more stable than α helices until Ala18. Additionally, the unconstrained optimization of polyalanine peptides from Ala4 to Ala18 started from ideal α conformations produces almost exclusively 3_{10} helices.^{37–39} Other studies^{14,15,40} have shown that the addition of an empirical vdW correction to B3LYP greatly stabilizes the α helix, not only relative to the fully extended peptide but also relative to the 3_{10} helix.

In this work we assess the performance of the B97-D functional against RHF, B3LYP, and MP2 in predicting the relative stability of α and 3_{10} helices for short alanine peptides, i.e., from Ala4 to Ala16. In agreement with previous calculations,^{13,14} our results show that the inclusion of a dispersion correction does indeed affect the relative stability of helical motifs in the gas phase, with the B97-D results being the closest to the MP2 reference calculations. The data from this analysis will be particularly useful for assessing the performance of existing protein force fields for gas-phase modeling, and may also serve as a benchmark for any revision of the force field.^{8,41–43}

Computational method

The alanine dipeptide was built with Argus Lab⁴⁴ in a conformation close to the known global minimum C7eq geometry, and its structure was fully optimized at the B97-D//def2-TZVP level of theory. N and C termini were capped with ACE and NMe groups. The Ramachandran plot shown in Fig. 1 was obtained by optimizing all degrees of freedom except for the $\phi\psi$ backbone torsion angles, which were scanned in 20° steps. The minima were identified by performing an unrestrained optimization of structures near low-energy areas found in the Ramachandran plot. All B97-D calculations were performed with v.6 of TURBOMOLE⁴⁵ with the def2-TZVP basis set, included in the TURBOMOLE basis set library. The choice of such extended AO basis set has been shown to minimize the BSSE error to a negligible level.^{20,46} All B97-D calculations were done within the resolution-of-the-identity (RI) approximation for the Coulomb term.^{47–49} All geometry optimizations have been carried out in terms of internal redundant coordinates.

The polyalanine structures were built with Argus Lab⁴⁴ in near ideal conformations. N and C termini were capped with ACE and NMe groups. The α and 3_{10} helices were obtained by geometry optimization at the RHF//6–311G(d,p) level of all degrees of freedom, except for the peptide backbone $\phi\psi$ torsion angles, which were constrained to match the following target values: $\phi = 57^\circ$, $\psi = 47^\circ$ for α helices, and $\phi = -49^\circ$, $\psi = -26^\circ$ for 3_{10} helices. The ideal helical conformations obtained were used for single-point energy calculations and as starting conformations for unconstrained geometry optimizations. Single point energies were calculated at the B97-D//def2-TZVP, RHF//6–311++G(2d,2p), B3LYP//6–311++G(2d,2p), and MP2//6–31G(d) levels of theory. These basis sets have been chosen based on the

feasibility of the calculation for all the peptides tested. Nevertheless, we only tested triple-zeta quality basis sets for the smallest peptide (Ala4) with larger shells of polarization functions, such as 6-311++G(3df,3pd), in combination with RHF and B3LYP and the 6-311++G(2d,2p) basis set in combination with MP2. Not surprisingly for Ala4, the energy differences obtained for RHF and B3LYP with different basis sets were very small, i.e., in the order of 0.2 kcal/mol (1 cal = 4.184 J). We may have observed larger differences for longer peptides, yet the calculations would have been prohibitively long. Larger differences in the order of 1.7 kcal/mol were observed for the MP2 calculations with the 6-31G(d) and 6-311++G(2d,2p) basis sets. Nevertheless, the use of a basis set larger than 6-31G(d) would have made the MP2 calculation unfeasible for larger peptides. Additionally, previous calculations⁵⁰ on polyalanine from Ala1 to Ala7, carried out with MP2//6-31 G(d) and with MP2//cc-pVDZ, show rather small energy differences. All calculations, except for the B97-D//def2-TZVP that was done with TURBOMOLE, were done with Gaussian 09.⁵¹

Results and discussion

Alanine dipeptide (Ala2)

The Ramachandran plot shown in Fig. 1 was obtained by scanning the Ala2 $\phi\psi$ torsional space in 20° steps at the B97-D//def2-TZVP level of theory. Full geometry optimization of the structures, corresponding to shallow areas of the plot, allowed us to locate 6 minima, and these structures are shown in Fig. 2. The same minima have been identified and characterized previously in gas phase by means of QM methods.¹¹ Torsion angles and relative energies are shown in Tables 1 and 2, respectively. The 3 most stable minima, i.e., C7eq, C5, and C7ax, are clearly visible on the map in Fig. 1, while the other 3, i.e., (β 2, α L, and α'), are located on more leveled areas of the potential energy surface. In Table 2, the B97-D//def2-TZVP relative energies are compared to MP2//aug-cc-dVPZ and MP2//CBS limit calculations, with the latter providing the best reference set available for this particular system.¹¹ In agreement with previous gas-phase calculations done at various level of theory,^{11,52} C7eq is the global minimum. The graph in Fig. 3 shows that the energies of the minima obtained at the B97-D//def2-TZVP level deviate from the MP2//aug-cc-dVPZ values by an average of 0.23 kcal/mol, with the largest deviations associated to the α L and α' conformations (see also Table 2). The B97-D//def2-TZVP calculations perform quite well even when compared with the MP2//CBS limit. Indeed, as shown in Fig. 3, the B97-D//def2-TZVP results deviate from the reference by an average of 0.41 kcal/mol, with the largest deviations associated to the C7ax and α' conformations. Nevertheless, these differences are still quite small, with ΔE between B97-D//def2-TZVP and the MP2//CBS limit of 0.62 kcal/mol for the C7ax and 0.63 kcal/mol for the α' conformation. As for the MP2//aug-cc-dVPZ results, the largest difference between the B97-D//def2-TZVP calculation and the MP2//CBS limit is in the relative stability between the C5 and C7ax minima, with the C5 conformer more stable than the C7ax at the MP2//CBS limit by 1.27 kcal/mol. At the B97-D//def2-TZVP and also at the MP2//aug-cc-dVPZ levels, the energy gap is much smaller, with $\Delta E = 0.34$ and 0.09 kcal/mol, respectively.

The hydrogen bonding parameters for all minima are shown in Table 3. The largest contribution to the stability of the minima comes from two types of hydrogen bonding

interactions, one between the oxygen of the carboxylate and the nitrogen of the amide group ($N\cdots O$) and the other between the nitrogen atoms of the two amide groups ($N\cdots H\cdots N$).⁵³ Here, we are not considering hydrogen bonds between a C-H donor and the carboxylate oxygen, as in the absence of strong electron-withdrawing groups adjacent to the donor such interactions are rather weak⁵⁴ and most likely on the order of the calculation error. The hydrogen bonding data clarify the origin of the relative stabilities between the Ala2 minima. Indeed, the most stable conformations are all stabilized by short hydrogen bonds (see Fig. 2 and Table 3). The largest stability derives from hydrogen bonds involving the carbonyl oxygen, where the distance between donor and acceptor ranges between 1.9 and 2.5 Å, and the angle between donor-hydrogen-acceptor ranges between $180^\circ \pm 20^\circ$.⁵⁵ The C7eq structure obtained at the B97-D//def2-TZVP is stabilized by an internal hydrogen bond of 2.09 Å between the carboxylate oxygen and the peptide amide hydrogen (see also Fig. 2). C7ax is also stabilized by a hydrogen bond of 1.9 Å between the oxygen of the terminal carboxylate and the hydrogen of the terminal amide. As shown in Table 4, the $N\cdots H\cdots O$ hydrogen bonding parameters are quite similar to the ones obtained with MP2//aug-cc-pVDZ, with the B97-D data consistently overestimating the MP2 reference, with exception of αL . The $N\cdots H\cdots N$ hydrogen bonds parameters are virtually identical, as they are known to be less affected by the calculation method.¹¹ Nevertheless, the structures and energies obtained for $\beta 2$ and αL are known to depend quite distinctly on the level of theory, as, unlike the C7eq C5 and C7ax, the $\beta 2$ and αL minima are located on shallow areas of the Ramachandran plot.¹¹ As shown in Fig. 2 and Table 3, both $\beta 2$ and αL lack an effective $N\cdots H\cdots O$ hydrogen interaction but are stabilized by $N\cdots H\cdots N$ bonds relative to the α' conformation, which does not have any intramolecular hydrogen bonds. Steric hindrance is what separates the energies of the 3 most stable minima. More specifically, the unfavourable steric interaction between the methyl sidechain and the carboxylate and amide groups is what destabilized C7ax relative to C5 and to the global minimum C7eq.

Polyalanine peptides

The stability of a series of polyaniline peptides in α and 3_{10} helix conformations, see Fig. 4, were calculated relative to the fully extended peptides, i.e., $\phi = \psi = 180$. We chose to compare the performance of B97-D//def2-TZVP against RHF and B3LYP in combination with the 6-311G++(2d,2p) basis set, and against MP2 with a 6-31G(d) basis set. Due to the smaller size of the basis set, the MP2 calculations might be affected by intramolecular BSSE. Nevertheless, comparison of our MP2 data with the GEBF-MP2//6-311++G** calculations from Hua and co-workers¹⁴ and with the MP2//cc-pVDZ from Jagielska and Skolnick⁵⁰ indicate that the BSSE effect is small and that the relative stability trends obtained at the MP2//6-31G(d) level are correct. For simplicity, from now on all data will be indicated only by the name of the QM method (or functional) used to obtain them, without basis set specification. Results are shown in Figs. 5 to 7.

The results we obtained with B97-D are closest to the MP2 data set (see Fig. 5). This is in accord with previous work by Hua and co-workers,¹⁴ who showed good agreement between the behaviour of the M06-2X functional and MP2 also for polyaniline peptides. The M06-2X functional was designed to take into account nonlocal effects with the inclusion of double the amount of nonlocal exchange.²³ Contrary to the M06-2X vs. MP2 results that

show a small but noticeable energy difference even for the smallest peptides, the difference between the B97-D and MP2 results range from 0.1 to 5 kcal/mol up to Ala8, with an overall better agreement found for 3_{10} helices relative to α .

The relative stabilities of the helical motifs obtained with RHF and B3LYP shown in Figs. 6 and 7, clearly attest the influence of the dispersion energy contribution in gauging the polypeptides conformation. Indeed, both graphs show that as the number of residues increases, the contribution of the electron correlation in the stability of both helices becomes progressively larger. Dispersion forces contribute in the stabilization of both helices and in particular of the α L helices. This trend has been shown to progress unchanged for larger peptides up to Ala40.¹⁴

The B97-D results are in good agreement with MP2 also in regards to the relative stability of the helical motifs in the gas phase. Both data sets show that for short peptides the 3_{10} helix is the most stable conformation. As shown in Fig. 5, B97-D predicts a switch in stability between Ala8 and Ala10, while MP2 between Ala6 and Ala8. Even in the absence of solvent effects, these results show that the intrinsic stability of the helices in function of the peptide length justifies the average length of the α L and 3_{10} helices found in proteins. On the opposite end, the B3LYP results, shown in Fig. 6, predict that the 3_{10} helix is always more stable than the α helix. The switch occurs eventually at around Ala40.¹⁴ The use of a smaller basis as 6-31G(p,d) set with B3LYP recovers a switch in stability, with the α helix becoming more stable than the 3_{10} between Ala10 and Ala12 (data not shown). Nevertheless, with a smaller basis set the contribution of the basis set superimposition error (BSSE) may be non-negligible. Therefore, based on the fact that the effect of the BSSE depends of the type of secondary structure⁵⁶ and also considering the wrong behaviour of the B3LYP functional for this type of system, the switch observed for B3LYP//6-31G(d) could be due to a fortuitous cancellation of errors. The results obtained with RHF, shown in Fig. 7, are in better agreement with B97-D and MP2 than B3LYP, with a switch in stability between 3_{10} and α helices predicted between Ala12 and Ala14. The overall rate of stabilization for both helices in function of the peptide length is slightly higher than the one predicted by B3LYP, but not quite high as the stabilization effect predicted by B97-D and MP2.

Conclusions

In this work we show the effect of the inclusion of an empirical dispersion term in the conformational energy of Ala2 and in the prediction of the relative stabilities of polyaniline helical motifs. Our study has been carried out with the GGA corrected functional B97-D³⁵ and compared to MP2 calculations at different levels of theory, chosen based on the size of the system. Our results show that electron correlation has an effect on the conformational energy of peptides with a weight that increases with the peptide length. The conformational energies of the minima found for Ala2 are in very good agreement with the “golden standard” MP2//CBS limit calculations.¹¹ This result is particularly encouraging considering that the same MP2//CBS limit data have been also shown to correlate very well with CCSD(T) data obtained for a non-capped alanine dipeptide.⁵² Nevertheless, a comparison between the Ala2 conformational energy surface in the gas phase and the one obtained from

a survey of the Brookhaven Protein Data Bank⁵⁷ shows that of all the minima identified only the C5 conformation is sufficiently populated in both plots.⁵⁸ This result indicates clearly that Ala2 in the gas phase alone is an inadequate model for the development of empirical parameters for the protein backbone in the condensed phase, independently of the level of theory.⁵⁹ A large number of previous investigations^{58,60–62} indicate that the Ala2 conformation is strongly influenced by solvent. Indeed, the Ala2 conformational energy surface even with implicit hydration reflects much better the PDB-derived surface.^{63,64} Based on this information, our results indicate that the conformational propensity of the capped Ala2 model is indeed affected by correlation effects, but to a much lesser degree than it is affected by solvent effects.

As the size of the peptide increases the effect of dispersion on the peptide conformational energy becomes more and more significant. The B97-D//def2-TZVP calculations are in very good agreement with the MP2//6–31G(d) reference and with earlier work.¹⁴ Our results show that in gas phase 3_{10} helices are more stable than α only for small peptides, and that α becomes more stable for peptides larger than Ala10. This is also in agreement with data obtained from the PDB that shows that all 3_{10} helices found in proteins are rather short, the longest ones containing 7 to 11 residues. On the contrary, the results obtained with B3LYP indicate that the 3_{10} helix is always more stable than the α . RHL recovers the change in the relative stability of the helices in function of the size of the peptide; however the RHF results are in agreement with the B97-D//def2-TZVP calculations only qualitatively. In conclusion, our results in agreement with earlier work,^{14,50} suggest that the inclusion of electron correlation effects is essential for the correct prediction of the conformational propensity of larger peptides.

Acknowledgments

Funding from the Science Foundation of Ireland (08/IN.1/B2070), the European Research Development Fund, and the National Institutes of Health (GM094919 (EUREKA)) is gratefully acknowledged.

References

1. Smith DP, Knapman TW, Campuzano I, Malham RW, Berryman JT, Radford SE, Ashcroft AE. *Eur.J.MassSpectrom.* 2009; 15:113.
2. Chen L, Shao Q, Gao YQ, Russel DH. *J. Phys. Chem. A.* 2011; 115:4427. [PubMed: 21476523]
3. Calvo F, Chirof F, Albrieux F, Lemoine J, Tsybin YO, Pernot P, Dugourd P. *J. Am. Soc. Mass Spectrom.* 2012; 23:1279. [PubMed: 22573497]
4. Hamilton JV, Renaud JB, Mayer PM. *Rapid Commun. Mass Spectrom.* 2012; 26:1591. [PubMed: 22693114]
5. Gould IR, Cornell WD, Hillier IH. *J. Am. Chem. Soc.* 1994; 116:9250.
6. Head-Gordon T, Head-Gordon M, Frisch MJ, Brooks CL, Pople JA III. *J. Am. Chem. Soc.* 1991; 113:5987.
7. Momany FA, Klimkowski VJ, Schafer L. *J. Comp Chem.* 1990; 11:654.
8. Beachy MD, Chasman D, Murphy RB, Halgren TA, Friesner RA. *J. Am. Chem. Soc.* 1997; 119:5908.
9. Murphy RB, Pollard WT, Friesner RA. *J. Chem. Phys.* 1997; 106:5073.
10. Aleman C, Leon S. *J.Mol. Struct. THEOCHEM.* 2000; 505:211.
11. Vargas R, Garza J, Hay BP, Dixon DA. *J. Phys. Chem. A.* 2002; 106:3213.
12. Improta R, Vitagliano L, Esposito L. *PLoS One.* 2011; 6

13. Tkatchenko A, Rossi M, Blum V, Ireta J, Scheffler M. *Phys. Rev. Lett.* 2011;106.
14. Hua S, Xu L, Li W, Li S. *J. Phys. Chem. B.* 2011; 115:11462. [PubMed: 21859141]
15. Wu Q, Yang WT. *J. Chem. Phys.* 2002; 116:515.
16. Kaschner R, Hohl D. *J. Phys. Chem. A.* 1998; 102:5111.
17. Allen MJ, Tozer DJ. *J. Chem. Phys.* 2002; 117:11113.
18. Singh RK, Tsuneda T. *J. Comp. Chem.* 2012
19. Cohen AJ, Mori-Sanchez P, Yang WT. *Chem. Rev.* 2012; 112:289. [PubMed: 22191548]
20. Grimme S. *J. Comput. Chem.* 2004; 25:1463. [PubMed: 15224390]
21. Tkatchenko A, DiStasio RA Jr, Head-Gordon M, Scheffler M. *J. Chem. Phys.* 2009;131.
22. Tkatchenko A, Scheffler M. *Phys. Rev. Lett.* 2009;102.
23. Zhao Y, Truhlar DG. *Theor. Chem. Acc.* 2008; 120:215.
24. Grimme S. *J. Comput. Chem.* 2006; 27:1787. [PubMed: 16955487]
25. Hujo W, Grimme S. *J. Chem. Theory Comp.* 2011; 7:3866.
26. Hujo W, Grimme S. *Phys. Chem. Chem. Phys.* 2011; 13:13942. [PubMed: 21594296]
27. Lonsdale R, Harvey JN, Mulholland AJ. *J. Phys. Chem. Lett.* 2010; 1:3232.
28. Siegbahn PEM, Blomberg MRA, Chen S-L. *J. Chem. Theory Comput.* 2010; 6:2040.
29. Santoro S, Liao R-Z, Himo F. *J. Org. Chem.* 2011; 76:9246. [PubMed: 21978323]
30. Xu XF, Liu P, Lesser A, Sirois LE, Wender PA, Houk KN. *J. Am. Chem. Soc.* 2012; 134:11012. [PubMed: 22668243]
31. Osuna S, Swart M, Sola M. *J. Phys. Chem. A.* 2011; 115:3491. [PubMed: 21438570]
32. Grimme S, Antony J, Schwabe T, Mueck-Lichtenfeld C. *Org. Biomol. Chem.* 2007; 5:741. [PubMed: 17315059]
33. Jurecka P, Cerny J, Hobza P, Salahub DR. *J. Comput. Chem.* 2007; 28:555. [PubMed: 17186489]
34. Ehrlich S, Moellmann J, Grimme S. *Acc. Chem. Res.* 2012
35. Antony J, Grimme S. *Phys. Chem. Chem. Phys.* 2006; 8:5287. [PubMed: 19810407]
36. Long SB, Tao X, Campbell EB, MacKinnon R. *Nature.* 2007; 450:376. [PubMed: 18004376]
37. Wieczorek R, Dannenberg JJ. *J. Am. Chem. Soc.* 2004; 126:14198. [PubMed: 15506786]
38. Wieczorek R, Dannenberg JJ. *J. Am. Chem. Soc.* 2004; 126:12278. [PubMed: 15453756]
39. Wieczorek R, Dannenberg JJ. *J. Am. Chem. Soc.* 2003; 125:14065. [PubMed: 14611243]
40. Liu HY, Elstner M, Kaxiras E, Frauenheim T, Hermans J, Yang WT. *Protein. Struct. Funct. Genet.* 2001; 44:484.
41. Kaminski GA, Friesner RA, Tirado-Rives J, Jorgensen WL. *J. Phys. Chem. B.* 2001; 105:6474.
42. Kollman PA. *Acc. Chem. Res.* 1996; 29:461.
43. Hornak V, Abel R, Okur A, Strockbine B, Roitberg A, Simmerling C. *Proteins: Struct. Funct. Bioinf.* 2006; 65:712.
44. Thompson, MA. ACS meeting. Philadelphia, PA: 2004.
45. GmbH, FK., editor. 6.2 ed. University of Karlsruhe Karlsruhe; 2012.
46. Plumley JA, Dannenberg JJ. *J. Comp. Chem.* 2011; 32:1519. [PubMed: 21328398]
47. Baerends EJ, Ellis DE, Ros P. *Chem. Phys.* 1973; 2:41.
48. Dunlap BI, Connolly JWD, Sabin JR. *J. Chem. Phys.* 1979; 71:3396.
49. Vahtras O, Almlöf J, Feyereisen MW. *Chem. Phys. Lett.* 1993; 213:514.
50. Jagielska A, Skolnick J. *J. Comp. Chem.* 2007; 28:1648. [PubMed: 17342701]
51. Frisch, MJ.; Trucks, GW.; Schlegel, HB.; Scuseria, GE.; Robb, MA.; Cheeseman, JR.; Scalmani, G.; Barone, V.; Mennucci, B.; Petersson, GA.; Nakatsuji, H.; Caricato, M.; Li, X.; Hratchian, HP.; Izmaylov, AF.; Bloino, J.; Zheng, G.; Sonnenberg, JL.; Hada, M.; Ehara, M.; Toyota, K.; Fukuda, R.; Hasegawa, J.; Ishida, M.; Nakajima, T.; Honda, Y.; Kitao, O.; Nakai, H.; Vreven, T.; Montgomery, JA., Jr; Peralta, JE.; Ogliaro, F.; Bearpark, M.; Heyd, JJ.; Brothers, E.; Kudin, KN.; Staroverov, VN.; Kobayashi, R.; Normand, J.; Raghavachari, K.; Rendell, A.; Burant, JC.; Iyengar, SS.; Tomasi, J.; Cossi, M.; Rega, N.; Millam, JM.; Klene, M.; Knox, JE.; Cross, JB.; Bakken, V.; Adamo, C.; Jaramillo, J.; Gomperts, R.; Stratmann, RE.; Yazyev, O.; Austin, AJ.;

Cammi, R.; Pomelli, C.; Ochterski, JW.; Martin, RL.; Morokuma, K.; Zakrzewski, VG.; Voth, GA.; Salvador, P.; Dannenberg, JJ.; Dapprich, S.; Daniels, AD.; Farkas, Ö.; Foresman, JB.; Ortiz, JV.; Cioslowski, J.; Fox, DJ. Gaussian Inc. Wallingford CT: 2009.

52. Perczel A, Farkas O, Jakli I, Topol IA, Csizmadia IG. *J. Comput. Chem.* 2003; 24:1026. [PubMed: 12759903]
53. Kim KS, Friesner RA. *J. Am. Chem. Soc.* 1997; 119:12952.
54. Jones CR, Baruah PK, Thompson AL, Scheiner S, Smith MD. *J. Am. Chem. Soc.* 2012; 134:12064. [PubMed: 22789294]
55. Hubbard, R.; Kamran Heider, M., editors. *Hydrogen bonds in Proteins: Role and Strength.* Chichester: John Wiley and Sons; 2010.
56. Balabin RM. *Mol. Phys.* 2011; 109:943.
57. Bernstein FC, Koetzle TF, Williams GJB, Meyer EF, Brice MD, Rodgers JR, Kennard O, Shimanouchi T, Tasumi M. *J. Mol. Biol.* 1977; 112:535. [PubMed: 875032]
58. MacKerell, AD. *Protein Force Fields.* Chichester, UK: Wiley; 1998.
59. Mackerell AD, Feig M, Brooks CL. *J. Comput. Chem.* 2004; 25:1400. [PubMed: 15185334]
60. Chekmarev DS, Ishida T, Levy RM. *J. Phys. Chem. B.* 2004; 108:19487.
61. Drozdov AN, Grossfield A, Pappu RV. *J. Am. Chem. Soc.* 2004; 126:2574. [PubMed: 14982467]
62. Wang ZX, Duan Y. *J. Comput. Chem.* 2004; 25:1699. [PubMed: 15362127]
63. Anderson AG, Hermans J. *Protein. Struct. Funct. Genet.* 1988; 3:262.
64. Garcia-Prieto FF, Galvan IF, Aguilar MA, Martin ME. *J. Chem. Phys.* 2011:135.

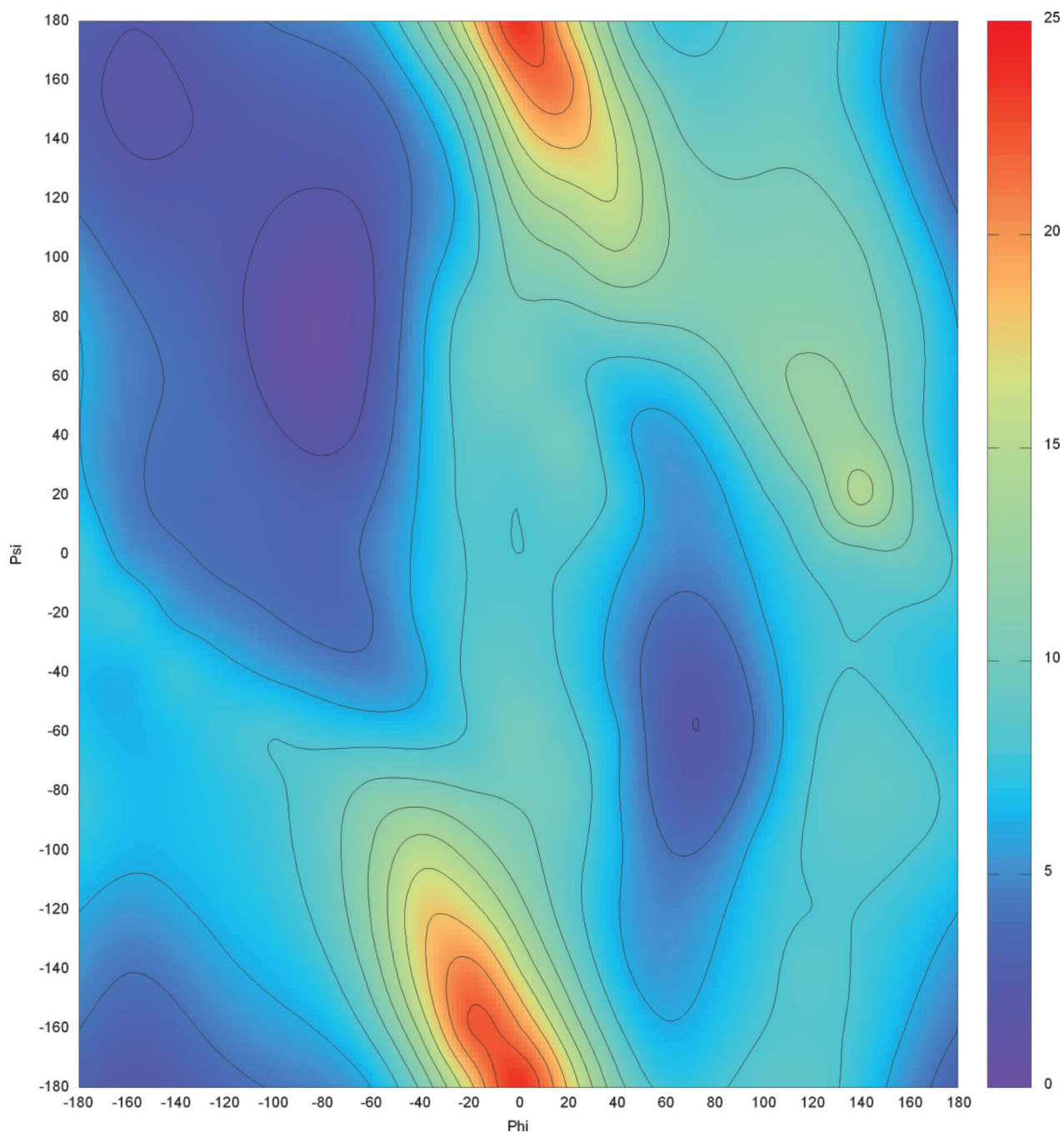


Fig. 1. Ramachandran plot for Ala2 calculated at the B97-D//def2-TZVP level of theory. Energies are in kcal/mol and the colouring scheme is defined in the bar on the right side of the plot. The contour lines are drawn at 2 kcal/mol levels for clarity.

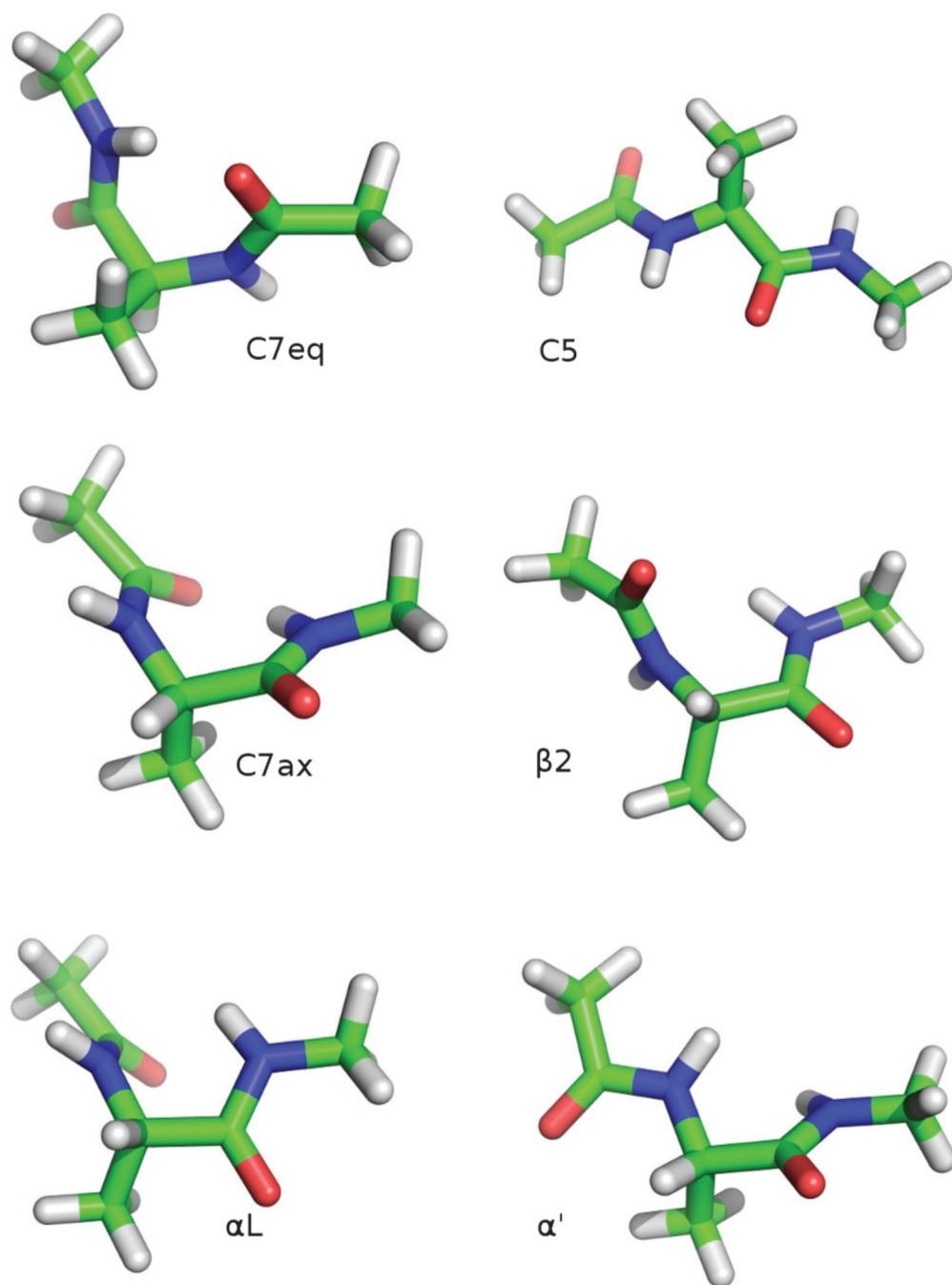


Fig. 2. Ala2 minima obtained at the B97D//def2-TZVP level of theory. Carbon atoms are shown in green (light grey in print version), nitrogen in blue (dark grey), oxygen in red (medium grey) and hydrogen in white.

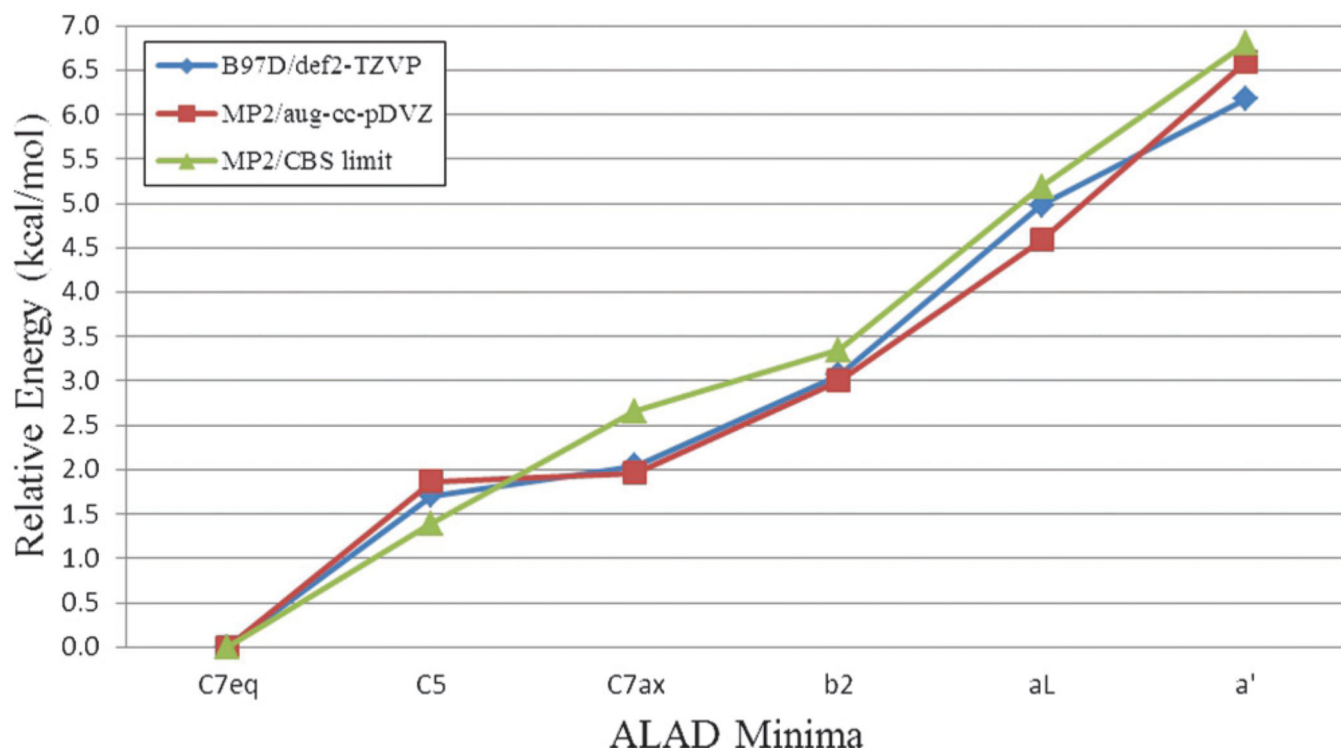


Fig. 3.
Relative stability of the Ala2 minima calculated at different levels of theory.

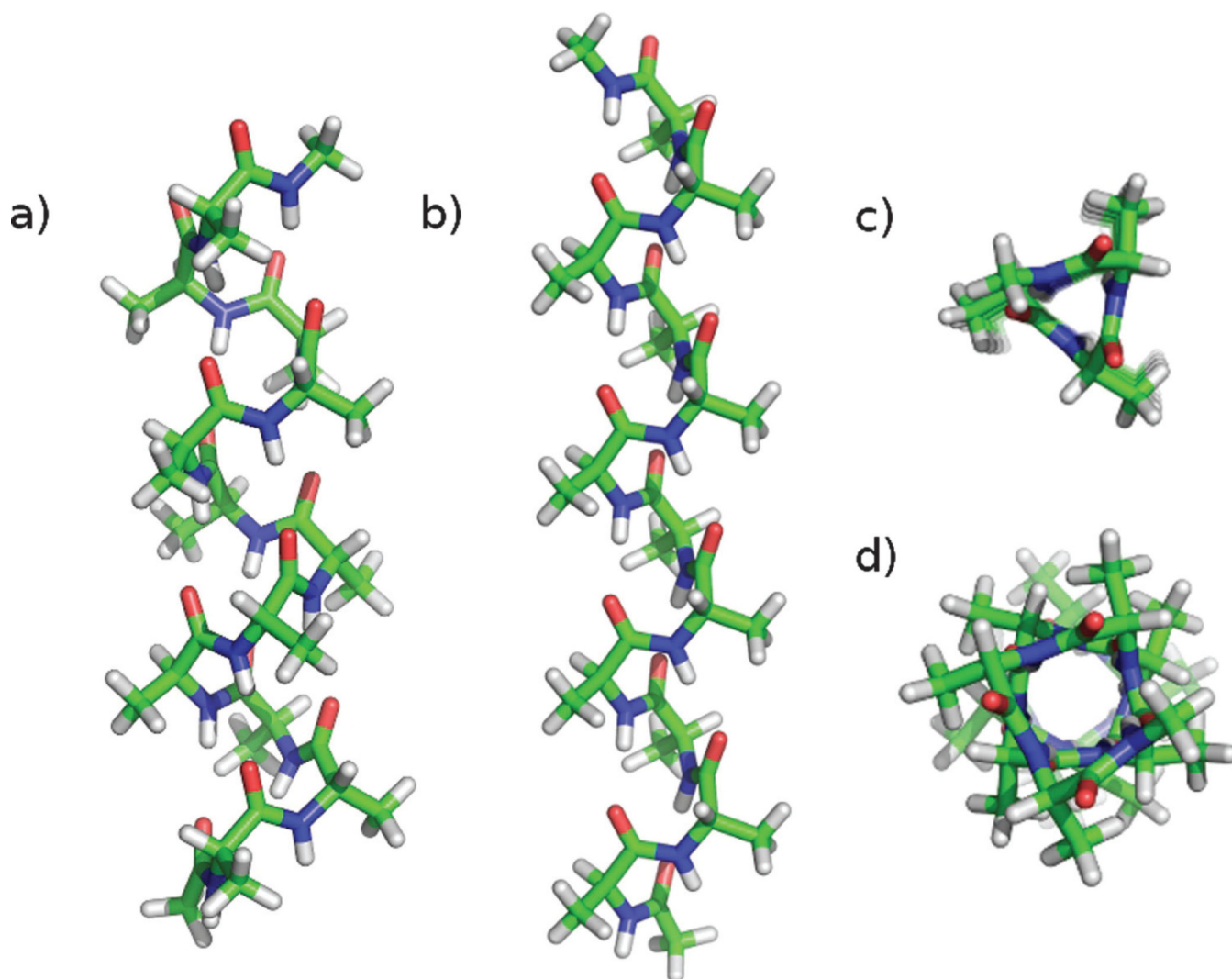


Fig. 4. Ideal helical conformations of Ala12: α and 3_{10} helices are shown in panel *a* and *b*, respectively; while the lumen of the 3_{10} and α helices is shown in panel *c* and *d*, respectively.

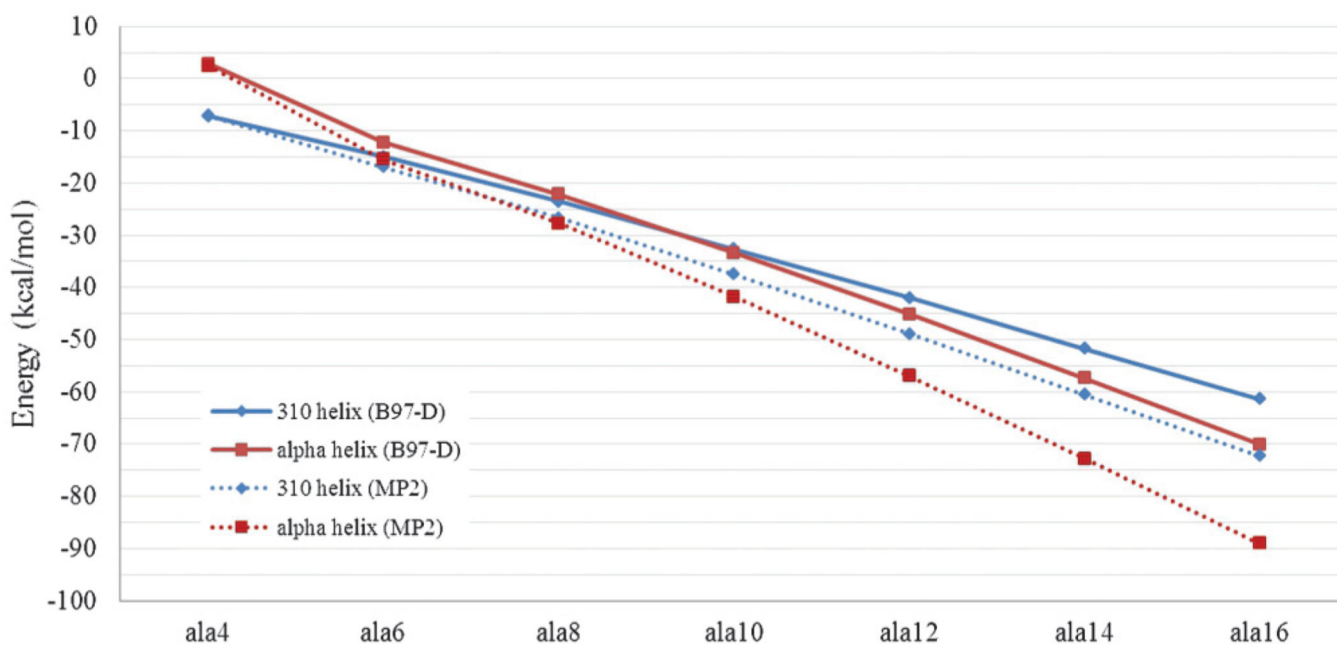


Fig. 5. Stability of α helices and 3_{10} helices in polyaniline peptides relative to the fully extended ($\phi = \psi = 180^\circ$) peptide conformation. Results obtained at the B97-D//def2-TZVP level are represented with solid lines, while results obtained at the MP2//6-31G* level are represented with dotted lines. Grid lines are drawn every 5 kcal/mol.

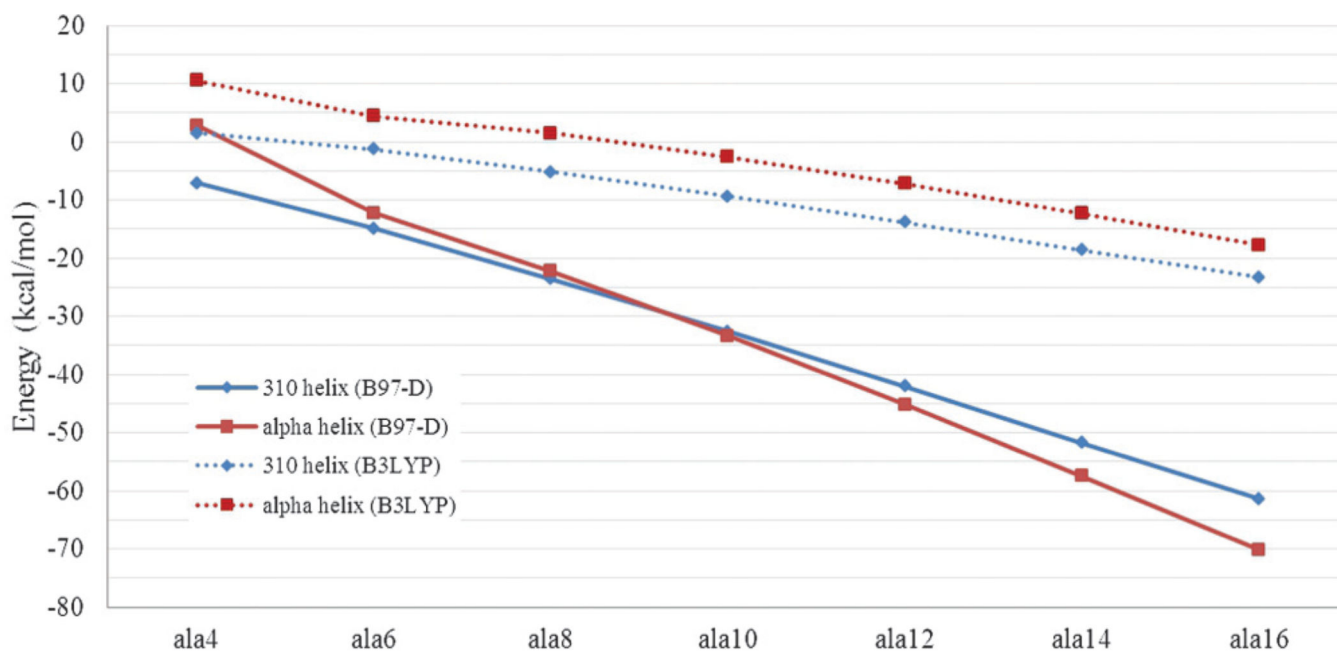


Fig. 6. Stability of α helices and 3_{10} helices in polyaniline peptides relative to the fully extended ($\phi = \psi = 180^\circ$) peptide conformation. Results obtained at the B97-D//def2-TZVP level are represented with solid lines, while results obtained at the B3LYP//6-311++G(2d,2p) level are represented with dotted lines. Grid lines are drawn every 5 kcal/mol.

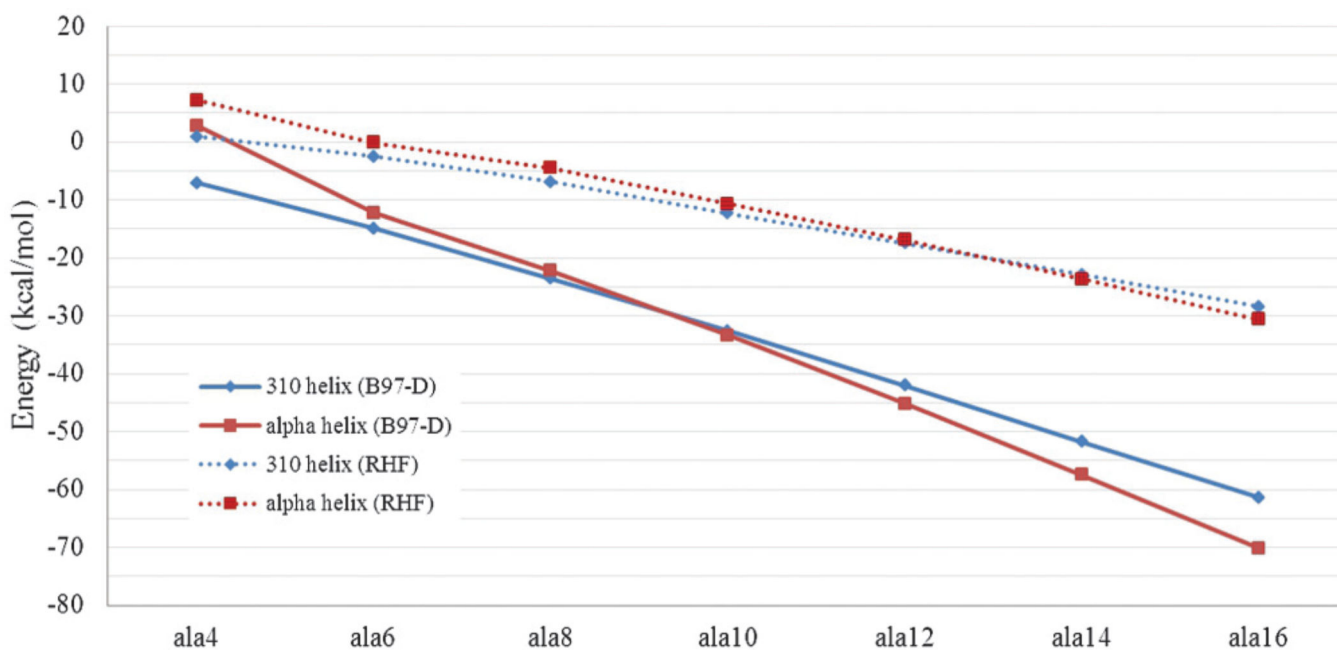


Fig. 7. Stability of α helices and 3_{10} helices in polyaniline peptides relative to the fully extended ($\phi = \psi = 180^\circ$) peptide conformation. Results obtained at the B97-D//def2-TZVP level are represented with solid lines, while results obtained at the RHF//6-311++G(2d,2p) level are represented with dotted lines. Grid lines are drawn every 5 kcal/mol.

Table 1

Dihedral angles defining the alanine dipeptide global and local minima obtained at different levels of theory.

Conformer	Dihedral angles	B97 D// def2-TZVP	MP2// aug-cc-pVDZ ^a
C7eq	ϕ	-82.3	-82.6
	ψ	75.4	75.8
C5	ϕ	-158.4	-161.1
	ψ	154.7	155.5
C7ax	ϕ	74.1	73.7
	ψ	-58.6	-53.7
β_2	ϕ	-93.5	-82.3
	ψ	4.8	-9.5
α_L	ϕ	69.2	63.8
	ψ	15.7	30.2
α'	ϕ	-165.6	-164.7
	ψ	-47.11	-38.3

^aRef. 11.

Table 2

Energies (in kcal/mol) of the alanine dipeptide minima calculated at different levels of theory.

Conformer	B97D// def2-TZVP	MP2// aug-cc-pVDZ ^a	MP2/CBS limit ^a
C7eq	0.00	0.00	0.00
C5	1.70 (0.17)	1.87 (0.48)	1.39
C7ax	2.04 (0.08)	1.96 (0.30)	2.66
β2	3.07 (0.07)	3.00 (0.35)	3.35
αL	4.98 (0.39)	4.59 (0.60)	5.19
α'	6.17 (0.42)	6.59 (0.21)	6.80

Note: The absolute deviation between the B97D//def2-TZVP and the MP2//aug-cc-pVDZ results is shown in parenthesis in the second column, while the absolute deviation between the MP2//aug-cc-pVDZ and the MP2//CBS limit data are shown in parenthesis in the third column.

^aRef. 11.

Table 3

Hydrogen bonding parameters for the alanine dipeptide minima obtained at the B97D//def2-TZVP level.

N–H···O=C Hydrogen Bond (B97 D//def2-TZVP)						
	C7eq	C5	C7ax	β2	αL	α'
Distance H···O	2.09	2.32	1.94	3.09	2.77	n/a
Distance N···O	2.97	2.74	2.88	3.65	3.24	n/a
Angle N–H···O	144.62	103.68	152.31	116.52	109.06	n/a
Angle H···O=C	103.42	83.20	103.11	61.03	68.74	n/a
N–H···N Hydrogen Bond (B97 D//def2-TZVP)						
Distance H···N	n/a	n/a	2.71	2.31	2.35	2.57
Distance N···N	n/a	n/a	3.01	2.78	2.81	2.84
Angle N–H···N	n/a	n/a	96.54	107.37	107.07	94.52

Note: Distances are shown in Å and angles in degrees. n/a indicates that the interaction is not present.

Table 4

Differences in the hydrogen bonding parameters of the minima shown in Table 3 relative to minima obtained at MP2//aug-cc-pVDZ level from Ref. 11.

<u>N-H...O=C Hydrogen Bond</u>						
	<u>C7eq</u>	<u>C5</u>	<u>C7ax</u>	<u>β2</u>	<u>αL</u>	<u>α'</u>
Distance H...O	0.07	0.09	0.06	0.14	-0.08	n/a
Distance N...O	0.06	0.06	0.06	0.25	0.11	n/a
Angle N-H...O	-0.18	-1.32	0.61	8.12	12.36	n/a
Angle H...O=C	-1.38	-1.5	-0.09	-2.37	1.24	n/a
<u>N-H...N Hydrogen Bond</u>						
Distance H...N	n/a	n/a	0.01	0.04	0.05	0.09
Distance N...N	n/a	n/a	0.04	0.03	0.04	0.08
Angle N-H...N	n/a	n/a	1.44	0.17	0.17	-0.48

Note: Negative values indicate that the MP2 distances (angles) are larger than the B97-D. Distances are shown in Å and angles in degrees. n/a indicates that the hydrogen bond is not present.